Hole spin coherence in a Ge/Si heterostructure nanowire

A. P. Higginbotham,[†,‡] T. W. Larsen,[†] J. Yao,[¶] H. Yan,[¶] C. M. Lieber,[¶,§]

C. M. Marcus,[†] and F. Kuemmeth[*,†]

E-mail: kuemmeth@nbi.dk

Supporting information for "Hole spin coherence in a Ge/Si heterostructure nanowire", is given on the following topics:

1. Acquisition method for Figure 1d

2. Image analysis

3. Clockwise T_1 pulse sequence (control experiment)

4. Theoretical estimate of T_2^* timescale for Ge/Si nanowire

[*]To whom correspondence should be addressed

[†]Center for Quantum Devices, Niels Bohr Institute, University of Copenhagen, 2100 Copenhagen, Denmark

[‡]Department of Physics, Harvard University, Cambridge, Massachusetts 02138, USA

[¶]Department of Chemistry and Chemical Biology, Harvard University, Cambridge, Massachusetts 02138, USA

[§]School of Engineering and Applied Sciences, Harvard University, Cambridge, Massachusetts 02138, USA

1. Acquisition method for Figure 1d

Data for Fig. 1d are acquired using a differential acquisition method, similar to that described in the main text. The RF carrier (frequency $\approx$ 830 MHz) is turned on and off at a rate of 157 Hz, and the reflected RF signal, demodulated by homodyne mixing, is fed into a SR830 lock-in amplifier. The output amplitude of the lock-in amplifier is then denoted as V_{RF}. In addition, the plunger gates are pulsed in a square wave along the detuning axis on a microsecond timescale. The fast pulses, designed to search for Pauli blockade (not discussed here), do not alter the stability diagram.

2. Image analysis

Software post-processing is done in three steps. First, the colorscale of images in Figures 2-4 are scaled to take into account different duty cycles of the differen pulse sequences, by multiplying each pixel by $\tau_{\Sigma}/\tau_{\mathrm{M}}$ where τ_{Σ} is the total pulse sequence length. Second, a constant voltage is subtracted from each image such that $V_{\mathrm{RF}} = 0$ corresponds to Coulomb blockade. Finally, we removed a glitch at $V_{\mathrm{R}} \approx 196$ mV by subtracting a suitable background near $V_{\mathrm{R}} = 196$ mV. This glitch occured whenever the DC component of V_{R} crossed 196 mV, independent of V_{L}. At this plunger gate voltage, data acquisition briefly paused while new calibrated plunger voltage values were loaded into the DC voltage source. This lookup process caused a small voltage spike in V_{RF} that does not represent any properties of the device itself.

Cuts along the V_{ε} axis in Fig. 3 and Fig. 4 are taken in software and numerically smoothed to remove pixelation errors.

3. Clockwise T_1 pulse sequence (control experiment)

Preparing a double quantum dot state by pulsing from E1 and E2 in (m+2, n+1) to P in (m+2, n) will initialize a singlet-correlated state at P [Fig. S1]. Only the singlet-singlet

interdot transition is observed, consistent with Pauli blockade for the counterclockwise pulse.

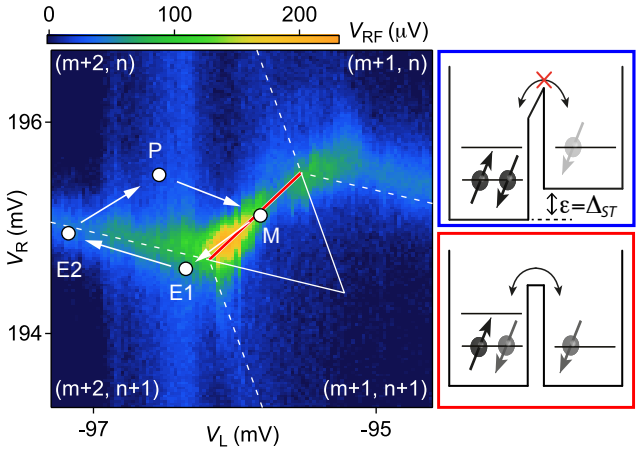

Figure S1: Reversed T_1 pulse sequence. V_{RF} at the measurement point $\mathrm{M} = (V_{\mathrm{L}}, V_{\mathrm{R}})$ of the reversed, cyclical Pauli blockade pulse sequence, indicated by white arrows. The pulse diagram has been scaled by a factor of 0.8 to fit on the plot. Dashed lines estimate changes in double dot hole occupancy (m, n), where m (n) denotes the occupancy of the left (right) dot. Large solid triangle outlines the region over which direct interdot charge transitions can occur.

4. Theoretical estimate of T_2^* for Ge/Si nanowire

In this section we present a theoretical estimate of the timescale of hole spin dephasing due to dipolar hyperfine coupling. The dephasing time is set by the dipolar coupling constant for the ^{73}Ge isotope, A_h^{Ge}, which is not well known. We estimate its magnitude using the contact hyperfine constant in GaAs, A_e^{GaAs}, determined by spin qubit dephasing times in these systems.

$T_2^* = \sqrt{2}h/\sigma$ is related to the nuclear hyperfine coupling constants by[1]

$$\sigma^2 = \frac{1}{4N}\sum_j v_j I^j (I^j + 1)(A^j)^2, \tag{S1}$$

where the sum is over the nuclear species with abundance v_j and spin I^j, and N is the total number of nuclei overlapped by the hole wavefunction. The wavefunction amplitude is assumed to be homogeneous at each nuclear site. Because all isotopes of Ga and As have

$I^j = I^{\mathrm{GaAs}} = 3/2$, Eq. (S1) can be rewritten as

$$\sigma^2 = \frac{1}{4N} I^{\mathrm{GaAs}}(I^{\mathrm{GaAs}}+1)\sum_j v_j (A_e^j)^2 = \frac{1}{4N} I^{\mathrm{GaAs}}(I^{\mathrm{GaAs}}+1)(A_e^{\mathrm{GaAs}})^2, \tag{S2}$$

where the last equality defines A_e^{GaAs}. In GaAs $T_2^* = 10{-}30$ ns,[2–5] implying $A_e^{\mathrm{GaAs}} = 200{-}600$ μeV assuming 10^6 nuclei.

We assume that $A_e^{\mathrm{GaAs}} \approx A_e^{\mathrm{Ge}}$ because both result from contact hyperfine interaction in $4s$ orbitals, and use the approximate scaling factor from Fischer et al[1] to estimate A_h^{Ge}:

$$\frac{A_h}{A_e} = \frac{1}{5}\left(\frac{Z_{\mathrm{eff}}(Ge,4p)}{Z_{\mathrm{eff}}(Ge,4s)}\right)^3. \tag{S3}$$

The ratio of effective nuclear charges is $\frac{Z_{\mathrm{eff}}(Ge,4p)}{Z_{\mathrm{eff}}(Ge,4s)} = 0.84$.[6] $A_e^{\mathrm{Ge}} = 200{-}600$ μeV then implies $A_h^{\mathrm{Ge}} = 20{-}70$ μeV. Eq. (S3) agrees with experimental measurements in III/V semiconductor dots to within 10-20 %.[7,8] σ is then calculated using Eq. (S1), assuming $N = 3\times10^5$ (dot length 80 nm) and the natural abundance values 0.92 for $I=0$ (^{70}Ge, ^{72}Ge, ^{74}Ge) and 0.08 for I=9/2 (^{73}Ge). This gives $\sigma = 25{-}90$ neV.

The expected dephasing time for holes confined in the germanium core of our devices is therefore $T_2^* = \frac{\sqrt{2}\hbar}{\sigma} = 65{-}230$ ns, in agreement with the experimental value $T_2^* = 180$ ns. We emphasize that this estimate is rough. In particular the actual size of both GaAs and Ge dots are not well known, which introduces uncertainty in our estimate for N.

References

(1) Fischer, J.; Coish, W. A.; Bulaev, D. V.; Loss, D. *Phys. Rev. B* **2008**, *78*, 155329.

(2) Petta, J. R.; Johnson, A. C.; Taylor, J. M.; Laird, E. A.; Yacoby, A.; Lukin, M. D.; Marcus, C. M.; Hanson, M. P.; Gossard, A. C. *Science* **2005**, *309*, 2180–2184.

(3) Koppens, F.; Buizert, C.; Tielrooij, K.-J.; Vink, I. T.; Nowack, K. C.; Meunier, T.; Kouwenhoven, L. P.; Vandersypen, L. *Nature* **2006**, *442*, 766–771.

(4) Barthel, C.; Reilly, D. J.; Marcus, C. M.; Hanson, M. P.; Gossard, A. C. *Phys. Rev. Lett.* **2009**, *103*, 160503.

(5) Medford, J.; Beil, J.; Taylor, J. M.; Bartlett, S. D.; Doherty, A. C.; Rashba, E. I.; DiVincenzo, D. P.; Lu, H.; Gossard, A. C.; Marcus, C. M. *Nat. Nanotechnol.* **2013**, *8*, 654–659.

(6) Clementi, E.; Raimondi, D. L. *J. Chem. Phys.* **1963**, *38*, 2686–2689.

(7) Chekhovich, E. A.; Krysa, AB,; Skolnick, M. S.; Tartakovskii, A. I. *Phys. Rev. Lett.* **2011**, *106*, 027402.

(8) Pribiag, V. S.; Nadj-Perge, S.; Frolov, S. M.; van den Berg, J. W. G.; van Weperen, I.; Plissard, S. R.; Bakkers, E. P. A. M.; Kouwenhoven, L. P. *Nat. Nanotechnol.* **2013**, *8*, 170–174.